

Fairing Triangular B -splines of Arbitrary Topology

Ying He, Xianfeng Gu, and Hong Qin

Center for Visual Computing (CVC) and Department of Computer Science
Stony Brook University, Stony Brook, NY, 11794-4400

e-mail: {yhe|gu|qin}@cs.sunysb.edu

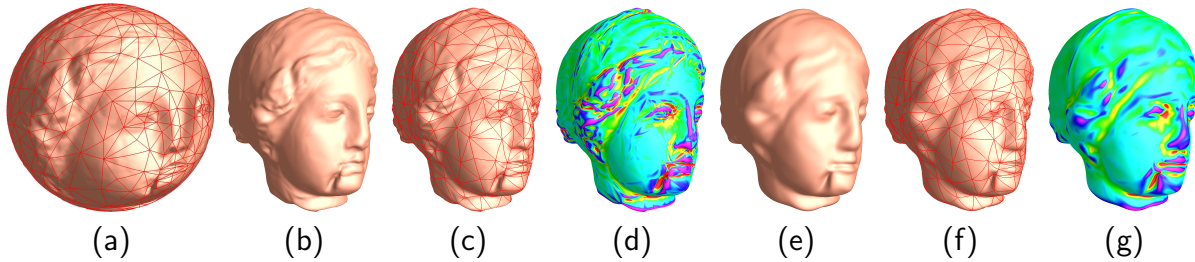


Figure 1: Fairing a spherical triangular B -spline. (a) shows the spherical domain with 682 triangles. (b), (c) and (d) shows a degree 5 (C^4 continuous) spherical spline and its mean curvature plot (red, $H < 0$, cyan, $H > 0$, green, $H \approx 0$). Note that the spline surface has high curvature concentration along the image of edges of the spherical triangles. (e), (f) and (g) shows the spline generated by our automatic fairing method. The computational time is only 8 seconds on a 3GHz Pentium IV PC. Compared to the surface in (b), the shape of the smooth spline (e) does not change too much, but the curvature distribution improves significantly. The red curves in (c) and (f) correspond to the edges in the spherical triangulation.

ABSTRACT

Triangular B -splines are powerful and flexible in modeling a broader class of geometric objects defined over arbitrary, non-rectangular domains. Despite their great potential and advantages in theory, practical techniques and computational tools with triangular B -splines are less-developed. This is mainly because users have to handle a large number of irregularly distributed control points over arbitrary triangulation. In this paper, we propose an automatic and efficient method to generate visually pleasing, high-quality triangular B -splines of arbitrary topology. Our experimental results on several real datasets show that triangular B -splines are powerful and effective in both theory and practice.

Keywords: Triangular B -splines, fairing algorithm

1 INTRODUCTION AND MOTIVATION

Triangular B -splines, introduced by Dahmen, Micchelli, and Seidel [5], are emerging as a novel and powerful tool for shape modeling and interactive graphics, because they can represent, without any degeneracy, complex geometric surfaces defined on open and irregular parametric domains. Using triangular B -splines, or triangular NURBS (the rational generalization of triangular B -splines), users can represent shapes over triangulated planar domains with lower-degree piecewise polynomials (rather than frequently-used tensor-product sur-

face construction over regular domains) that nonetheless maintain higher-order continuity across the boundary of their piecewise patchwork. Prior results have proved that any piecewise polynomial surface over a planar triangulation can be accurately represented in triangular B -splines. Triangular B -splines are even more powerful when being extended and generalized to spherical domain [32, 22] and manifold of arbitrary topology [17]. Therefore, triangular B -splines can potentially serve as a geometric standard for product data representation and model conversion in shape design and geometric processing.

Despite their aforementioned geometric advantages and modeling potential over popular tensor-product splines, triangular B -splines have not been widely used in research community and CAD industry. This is mainly because 1) users must deal with a large number of irregularly-distributed control points and their companion knots to make certain non-intuitive decisions on their placements; 2) Triangular B -splines have the so-called knot lines, where the surface curvature distribution along the curved triangular boundaries (corresponding to the edges in the domain triangulation) is much worse than other regions. There exist no effective approaches to control the overall curvature distribution and improve the shape quality via automatic control-point adjustment.

To overcome these shortcomings of triangular B -splines, this paper develops an automatic algorithm to generate visually pleasing triangular B -splines without the

need of any tedious manual operation on control points. Moreover, unlike the existing, classical fairing algorithms, which usually involve the expensive computation of physics-based fair functionals (such as membrane or thin-plate energy), our method solves a simple least square with linear constraints. Therefore, our approach is both fast and robust. Furthermore, our approach works for planar, spherical, and manifold triangular B -splines without any theoretical difficulties. Figure 1 shows an example generated using our automatic shape-fairing algorithm. The input is a C^4 spherical triangular B -spline (shown in (b)) with 682 domain triangles (shown in (a)). Pay attention to the spline surface marked with red curves which correspond to the edges of spherical triangulation (shown in (c)), and the mean curvature plot (shown in (d)), the spline surface have high curvature concentrations along the image of edges of the underlying domain triangulation. After automatic fairing, the overall shape only undergoes a small variation (in fact, the shape deviation from the original one is minimized), but the curvature distribution improves significantly (shown in (e),(f),(g)).

The remainder of this paper is organized as follows. Section 2 reviews the related work on simplex splines and triangular B -splines. Section 3 documents the theoretical background for planar, spherical, and manifold triangular B -splines. Section 4 presents the algorithm to construct smooth triangular B -splines. Section 5 shows our experimental results. Finally, we conclude the paper in Section 6.

2 PREVIOUS WORK

This section briefly surveys some related work in simplex splines and triangular B -splines.

The theoretical foundation of triangular B -splines lies in the multivariate B -spline, or simplex spline, introduced by de Boor [8] in 1976. Since then, many researchers have tried to produce useful linear combinations of simplex splines sharing some of the properties of the univariate B -splines, in particular, the polynomial or piecewise polynomial reproduction property (see [4] for a survey of simplex splines). Dahmen and Micchelli [6, 7] and Höllig [24], using combinatorial arguments, proposed convenient basis of simplex splines that reproduce polynomials of degree n . But the reproduction of C^{n-1} piecewise polynomial functions on a given triangulation could not be settled.

Based on the blossom or polar form [33] and B -patch [34], Dahmen, Micchelli and Seidel [5] proposed a general spline scheme in s -dimensional space, which

constructs a collection of multivariate B -splines whose linear span comprises all polynomials of degree no more than n . The bivariate case is called triangular B -spline or DMS spline. Due to its elegant construction and many attractive properties for geometric modeling, triangular B -spline has received much attention since its inception. Fong and Seidel [11] presented the first prototype implementation of triangular B -splines and show several useful properties, such as affine invariance, convex hull, locality, and smoothness. Greiner and Seidel [16] showed the practical feasibility of multivariate B -spline algorithms in graphics and shape design. Pfeifle and Seidel [31] demonstrated the fitting of a triangular B -spline surface to scattered functional data through the use of least squares and optimization techniques. Gormaz and Laurent studied the piecewise polynomial reproduction of triangular B -spline and give a direct and intuitive proof [15]. Franssen *et al.* [12] proposed an efficient evaluation algorithm, which works for triangular B -spline surfaces of arbitrary degree. He and Qin [23] presented a method of surface reconstruction using triangular B -splines with free knots. Recently, Neamtu [30] described a new paradigm of bivariate simplex splines based on the higher degree Delaunay configurations.

Traditional triangular B -splines are defined on the planar domains. Many researchers have explored the feasible ways to generalize them to be defined on sphere and manifold with arbitrary topology. Alfeld, Neamtu and Schumaker [1] presented spherical barycentric coordinates which naturally lead to the theory of Spherical Bernstein-Bézier polynomials (SBB). They showed fitting scattered data on sphere-like surfaces with SBB in [2]. Pfeifle and Seidel [32] presented scalar spherical triangular B -splines and demonstrated the use of these splines for approximating spherical scattered data. Neamtu [29] constructed a functional space of homogeneous simplex splines and showed that restricting the homogeneous splines to a sphere gives rise to the space of spherical simplex splines. He *et al.* [22] presented the rational spherical spline for genus zero shape modeling.

Recently, Gu, He and Qin [17] developed a general theoretical framework of manifold splines in which the existing spline schemes defined over planar domains can be systematically generalized to any manifold domain of arbitrary topology (with or without boundaries) using affine structures. They demonstrated the idea of manifold spline using triangular B -splines because of the attractive properties of triangular B -splines, such as arbitrary triangulation, parametric affine invariance, and piecewise polynomial reproduction [17].

All the existing literatures of triangular B -splines focus on either theoretical foundation or evaluation/data fitting

algorithms. No previous work has been done in the surface quality analysis of triangular B -splines. This paper aims at providing such tools for automatic shape control and analysis of triangular B -splines.

3 TRIANGULAR B -SPLINES

This section presents the construction of planar triangular B -splines, spherical triangular B -splines and manifold triangular B -splines, and summaries their properties in geometric design.

3.1 Planar triangular B -spline

The planar triangular B -spline is proposed by Dahmen, Micchelli and Seidel [5]. Their construction is as follows: let points $\mathbf{t}_i \in \mathbb{R}^2$, $i \in \mathbb{N}$, be given and define a triangulation

$$T = \{\Delta(I) = [\mathbf{t}_{i_0}, \mathbf{t}_{i_1}, \mathbf{t}_{i_2}] : I = (i_0, i_1, i_2) \in \mathcal{I} \subset \mathbb{N}^2\}$$

of a bounded region $D \subseteq \mathbb{R}^2$. Next, with every vertex \mathbf{t}_i of T , we associate a cloud of knots $\mathbf{t}_{i,0}, \dots, \mathbf{t}_{i,n}$ such that $\mathbf{t}_{i,0} = \mathbf{t}_i$. To clarify our explanation, we call $\{\mathbf{t}_{i,0} | i \in \mathbb{N}\}$ the primary knots and $\{\mathbf{t}_{i,j} | i \in \mathbb{N}, 1 \leq j \leq n\}$ the sub-knots. For every triangle $I = [\mathbf{t}_{i_0}, \mathbf{t}_{i_1}, \mathbf{t}_{i_2}] \in T$, we require

1. all the triangles $[\mathbf{t}_{i_0, \beta_0}, \mathbf{t}_{i_1, \beta_1}, \mathbf{t}_{i_2, \beta_2}]$ with $\beta = (\beta_0, \beta_1, \beta_2)$ and $|\beta| = \sum_{i=0}^2 \beta_i \leq n$ are non-degenerate.

2. the set

$$\text{interior}(\cap_{|\beta| \leq n} X_\beta^I) \neq \emptyset \quad (1)$$

$$\text{where } X_\beta^I = [\mathbf{t}_{i_0, \beta_0}, \mathbf{t}_{i_1, \beta_1}, \mathbf{t}_{i_2, \beta_2}]$$

3. if I has a boundary edge, say, $(\mathbf{t}_{i_0}, \mathbf{t}_{i_1})$, then the entire area $[\mathbf{t}_{i_0,0}, \dots, \mathbf{t}_{i_0,n}, \mathbf{t}_{i_1,0}, \dots, \mathbf{t}_{i_1,n}]$ must lie outside of the domain.

Then triangular B -spline basis function N_β^I , $|\beta| = n$, is defined by means of simplex splines $M(\mathbf{u}|V_\beta^I)$ as

$$N(\mathbf{u}|V_\beta^I) = |d_\beta^I| M(\mathbf{u}|V_\beta^I)$$

where $V_\beta^I = \{\mathbf{t}_{i_0,0}, \dots, \mathbf{t}_{i_0,\beta_0}, \dots, \mathbf{t}_{i_2,0}, \dots, \mathbf{t}_{i_2,\beta_2}\}$ and

$$d_\beta^I = d(X_\beta^I) = \det \begin{pmatrix} 1 & 1 & 1 \\ \mathbf{t}_{i_0, \beta_0} & \mathbf{t}_{i_1, \beta_1} & \mathbf{t}_{i_2, \beta_2} \end{pmatrix}$$

Assuming (1), these B -spline basis functions can be shown to be all non-negative and to form a partition of unity. Then, the planar triangular B -spline is defined as

$$\mathbf{F}(\mathbf{u}) = \sum_{I \in T} \sum_{|\beta|=n} \mathbf{c}_{I,\beta} N(\mathbf{u}|V_\beta^I), \mathbf{u} \in \mathbb{R}^2 \quad (2)$$

where $\mathbf{c}_{I,\beta} \in \mathbb{R}^3$ are the control points. This spline is globally C^{n-1} if all the sets X_β^I , $|\beta| \leq n$ are affinely independent.

3.2 Spherical triangular B -spline

Pfeifle and Seidel successfully generalized the planar triangular B -splines to the spherical domain [32]. The construction procedure is similar to its planar counterpart.

Denote by $\mathbb{S}^2 = \{\mathbf{x} | \mathbf{x} \in \mathbb{R}^3, \|\mathbf{x}\| = 1\}$ a unit sphere. Let points $\mathbf{t}_i \in \mathbb{S}^2$, $i \in \mathbb{N}$, be given and define a spherical triangulation T . We associate the sub-knots $\mathbf{t}_{i,1}, \dots, \mathbf{t}_{i,n} \in \mathbb{S}^2$ for each vertex \mathbf{t}_i of T . Then the spherical triangular B -spline basis function N_β^I , $|\beta| = n$, is defined by means of spherical simplex splines $M(\mathbf{u}|V_\beta^I)$ as $N(\mathbf{u}|V_\beta^I) = |\det(X_\beta^I)| M(\mathbf{u}|V_\beta^I)$. A degree n spherical triangular B -spline surface \mathbf{F} over T is then defined as

$$\mathbf{F}(\mathbf{u}) = \sum_{I \in T} \sum_{|\beta|=n} \mathbf{c}_{I,\beta} N(\mathbf{u}|V_\beta^I), \mathbf{u} \in \mathbb{S}^2. \quad (3)$$

where $\mathbf{c}_{I,\beta} \in \mathbb{R}^3$ are the control points.

The differences between the spherical triangular B -spline and planar triangular B -spline are 1) the domain is a unit sphere and the edges of triangulation are great circles; 2) the basis functions $N(\mathbf{u}|V_\beta^I)$ are spherical simplex splines which are defined using spherical barycentric coordinates [1]; 3) because the domain is closed, we don't need to worry about the boundary knots; 4) the affine invariance and convex hull property do not hold for spherical triangular B -splines. However, the *rational* spherical triangular B -spline has the convex hull property due to the partition of unity of rational basis functions (see [22]).

3.3 Manifold triangular B -spline

In [17], Gu, He and Qin systematically built the theoretical framework of manifold spline, which locally is a traditional spline patch, but globally defined on the manifold. First, the manifold is covered by a special atlas, such that the transition functions are affine. Then, the knots are defined on the manifold and the evaluation of polar form is carried out on the charts. Although on different charts, the knots are different, the evaluation value is consistent and independent of the choice of charts. Furthermore, the existence of such atlas depends on the domain topology. This new paradigm unifies traditional subdivision surfaces and splines. The followings are the theoretical background manifold splines.

Definition [Manifold] A 2-dimensional manifold is a connected Hausdorff space M for which every point has a neighborhood U that is homeomorphic to an open set V of \mathbb{R}^2 . Such a homeomorphism $\phi : U \rightarrow V$ is called a coordinate chart. An atlas is a family of charts $\{U_\alpha, \phi_\alpha\}$ for which U_α constitutes an open covering of M .

The central issue of constructing manifold splines is that the atlas must satisfy some special properties in order to meet all the requirements for the evaluation independence of chart selection. In [17], Gu *et al.* showed that for a local spline patch, the only admissible parameterizations differ by an affine transformation. This requires that all the chart transition functions are affine.

Definition [Affine atlas] A 2-dimensional manifold M with an atlas $\{U_\alpha, \phi_\alpha\}$, if all chart transition functions

$$\phi_{\alpha\beta} := \phi_\beta \circ \phi_\alpha^{-1} : \phi_\alpha(U_\alpha \cap U_\beta) \rightarrow \phi_\beta(U_\alpha \cap U_\beta)$$

are affine, then the atlas is called an affine atlas, M is called an affine manifold.

Two affine atlases are *compatible* if their union is still an affine atlas. All the compatible affine atlases form an *affine structure* of the manifold (see Figure 2).

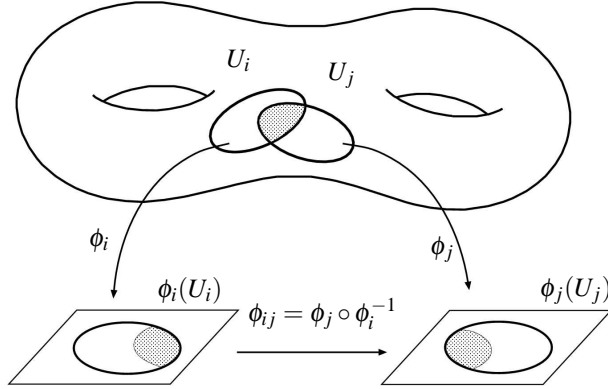


Figure 2: Affine manifold: The manifold is covered by a set of charts (U_i, ϕ_i) , where $\phi_i : U_i \rightarrow \mathbb{R}^2$. If two charts (U_i, ϕ_i) and (U_j, ϕ_j) overlap, the transition function $\phi_{ij} : \mathbb{R}^2 \rightarrow \mathbb{R}^2$ is defined as $\phi_{ij} = \phi_j \circ \phi_i^{-1}$. If all transition functions are affine, then the manifold is an affine manifold.

Definition [Manifold Spline] A manifold spline is a triple (M, C, F) , where M is the domain manifold with an atlas $\mathcal{A} = \{(U_\alpha, \phi_\alpha)\}$. C is the set of control points. F is a map $F : M \rightarrow \mathbb{R}^3$ representing the entire spline surface, such that

1. For each chart (U_α, ϕ_α) , the restriction of F on U_α is denoted as $F_\alpha = F \circ \phi_\alpha^{-1}$, a subset of control points C_α can be selected, such that $(\phi_\alpha(U_\alpha), C_\alpha, F_\alpha)$ form a planar spline patch.
2. The evaluation of F is independent of the choice of the local chart, namely, if U_α intersects U_β , then

$F_\alpha = F_\beta \circ \phi_{\alpha\beta}$, where $\phi_{\alpha\beta}$ is the chart transition function.

The geometric intuition of the above formal definition is that first we replace a planar domain by the atlas of the domain manifold, and then all the constituent spline patches naturally span across each other without any gap.

Theorem 1. The sufficient and necessary condition for a manifold M to admit manifold spline is that M must be an affine manifold.

This theorem implies that the existence of manifold splines solely depends on the existence of affine atlas. If the domain manifold M is an affine manifold, we will be able to directly generalize the local spline patches to a global spline defined on M .

Theorem 2. The only closed surface admitting affine atlas is of genus one. All oriented open 2-manifolds admit affine atlas.

Theorem 2 points out that not all surfaces admit the affine atlas. For closed surfaces, only genus-one surfaces have affine structures, but all surfaces with boundaries have affine structures. The topological obstruction of a global affine atlas is the Euler class. In fact, by removing one point from the closed domain manifold, we can convert it to an affine manifold.

Theorem 3 (Affine atlas deduced from conformal structure). Given a closed genus g surface M , and a holomorphic 1-form ω . Denote by $Z = \{\text{zeros of } \omega\}$ the zero points of ω . Then the size of Z is no more than $2g - 2$, and there exists an affine atlas on M/Z deduced by ω .

Essentially, Theorem 3 indicates that an affine atlas of a manifold M can be deduced from its conformal structure in a straightforward fashion.

Given a domain manifold M , a manifold triangular B -spline defined on M can be constructed as follows:

1. Compute the holomorphic 1-form basis for the domain mesh M using Gu-Yau's method [18].
2. Optimize the holomorphic 1-form ω to satisfy the uniformity criteria (see [26]).
3. Locate zero points Z of the holomorphic 1-form ω .
4. Compute the affine atlas of $M \setminus Z$ by integrating the holomorphic 1-form ω .
5. For each vertex $\mathbf{v}_i \in M \subset \mathbb{R}^3$, assign the sub-knots $\mathbf{t}_{i,j} \in M$, $j = 1, \dots, n$ to \mathbf{v}_i .

Similar to planar and spherical triangular B -spline (Equation (2) and (3)), the manifold triangular B -spline can be written in a similar fashion

$$\mathbf{F}(\mathbf{u}) = \sum_I \sum_{|\beta|=n} \mathbf{c}_{I,\beta} N(\mathbf{u}|V_\beta^I), \mathbf{u} \in M \quad (4)$$

where $\mathbf{c}_{I,\beta} \in \mathbb{R}^3$ are the control points. Given a parameter $\mathbf{u} \in M$, the evaluation can be carried out on arbitrary charts covering \mathbf{u} .

3.4 Properties of triangular B -splines

Triangular B -splines have many valuable properties which are critical for geometric and solid modeling. For examples, triangular B -splines are piecewise polynomial defined on the planar, spherical and manifold domain of arbitrary triangulation. Therefore, the computation of various differential properties, such as normals, curvatures, principal directions, are robust and efficient. The splines have local support, i.e., the movement of a single control point $\mathbf{c}_{I,\beta}$ only influences the surface on the triangle I and on the triangles directly surrounding I . The planar and manifold triangular B -splines are completely inside the convex hull of the control points. The rational spherical triangular B -splines also have convex hull property (see [22]). The degree n planar/spherical/manifold triangular B -splines are of C^{n-1} -continuous if there are no degenerate knots. Furthermore, by intentionally placing knots along the edges of the domain triangulation, we can model sharp features easily. The manifold spline of genus $g(\geq 1)$ has $2g - 2$ singular points while planar and spherical spline do not. Table 1 summaries the properties of triangular B -splines for geometric modeling.

4 FAIRING TRIANGULAR B -SPLINES

The problem of fairness is of central importance during the design process of free form surfaces. A fair surface is usually obtained by two different ways. The first one consists of modeling surfaces with fairness constraints: a physical based fairness criterion, such as thin-plate energy, is incorporated in the interpolation or approximation method. Another way to obtain fair surfaces is to apply a post-processing fairing method to a given surface. Most of the existing methods apply to meshes [36, 9, 10, 27], subdivision surfaces [21, 13], implicit surfaces [3], parametric surfaces, such as tensor-product B -splines [37, 28, 19, 20, 25]. However, no existing literature deals with fairing triangular B -spline surfaces. The goal of this paper is to present an efficient

post-processing fairing method for planar, spherical and manifold triangular B -splines.

Conventional methods for local and global fairing usually involve a physics based fairness criterion. Several frequently used examples are,

$$\iint_{\Omega} \mathbf{F}_u^2 + \mathbf{F}_v^2 dudv,$$

$$\iint_{\Omega} \mathbf{F}_{uu}^2 + 2\mathbf{F}_{uv}^2 + \mathbf{F}_{vv}^2 dudv.$$

All of the above fairness functionals involve the integration of the derivatives of \mathbf{F} over the parametric domain. Calculating the exact value of the fairness functional is challenging for triangular B -splines, since there is no restriction on the domain triangulation and the sub-knots are also distributed irregularly. A straightforward method is by domain clipping. For each domain triangle, we draw line segments by connecting any two knots. This line graph partitions the parametric domain into many regions, some of which may have very small angles. Note that on each region, the triangular B -spline is a single polynomial. Thus, the integration on each region can be computed by the quadrature-based methods. By adding the integral of all pieces, we get the value for the fairness functional of the whole parametric domain. This method works well for quadratic triangular B -spline [31], since the number of regions is small and its second order derivatives are constant. However, this method can not be directly applied to triangular B -splines with higher degree mainly because the number of integral regions increases dramatically and there exists many skinny regions which could cause serious numerical problems.

In this paper, we propose a new post-processing fairing method which does not need the computation of the complicated double integral. Instead, it only relies on a set of constraints which are linear of the control points.

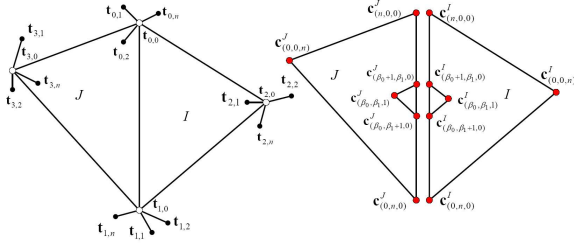
Our method is inspired by the seminal work of Gormaz *et al.* [15, 14] who studied the intrinsic property of triangular B -spline. Although triangular B -spline has C^{n-1} continuity if there are no degenerate knots, the spline surfaces may not as smooth as one expected. The curvature of the images of the edges in the parametric domain is larger than vicinity. Figure 4 shows a degree 4 triangular B -spline, which is C^3 -continuous everywhere. However, the surface is not smooth, because the high curvature concentrates along the edges of adjacent spline patches. This phenomenon is called ‘‘knot-line’’ of triangular B -splines.

In the following, we consider planar triangular B -spline. The same idea can be applied to spherical triangular B -spline and manifold triangular B -spline directly.

Table 1: Properties of triangular B -splines

	Arbitrary triangulation	Local control	Convex hull	Affine invariance	Smoothness	Singular points	Applications
Planar spline	yes	yes	yes	yes	$C^0 \sim C^{n-1}$	no	open surfaces, disk-topology
Spherical spline	yes	yes	no	no	$C^0 \sim C^{n-1}$	no	sphere-like, genus zero, closed surfaces
Manifold spline	yes	yes	yes	yes	$C^0 \sim C^{n-1}$	yes	surfaces of complicated topology

Given a degree n triangular B -spline surface $\mathbf{F}(\mathbf{u})$ defined on a planar triangulation T . Consider two domain triangles $\Delta(I) = [\mathbf{t}'_0, \mathbf{t}'_1, \mathbf{t}'_2] \in T$ and $\Delta(J) = [\mathbf{t}'_0, \mathbf{t}'_1, \mathbf{t}'_2] \in T$ such that $\Delta(I)$ and $\Delta(J)$ are adjacent. For example, suppose $\mathbf{t}'_0 = \mathbf{t}'_0$ and $\mathbf{t}'_1 = \mathbf{t}'_1$ (see Fig. 3). Therefore, the sub-knots satisfy $\mathbf{t}'_{0,i} = \mathbf{t}'_{0,i}$ and $\mathbf{t}'_{1,i} = \mathbf{t}'_{1,i}$, $i = 1, \dots, n$. Let $\mathbf{F}^I = \sum_{|\beta|=n} \mathbf{c}_{I,\beta} N(\mathbf{u}|V_\beta^I)$ be the polynomial on triangle I and similarly for \mathbf{F}^J . Let f^I and f^J be the polar forms of \mathbf{F}^I and \mathbf{F}^J , respectively (see [35] for the details of polar form). Then, Gormaz proved the following result [14] :

Figure 3: Illustration of Equation (5) for $r = 1$. Left, parametric domain; Right, control points.

The spline surface $\mathbf{F}(\mathbf{u})$ has no discontinuity of its n^{th} derivative along the lines

$$[\mathbf{t}'_{0,\beta_0}, \mathbf{t}'_{1,\beta_1}], \forall \beta, |\beta| = n, \beta_2 \leq r$$

if and only if

$$\mathbf{c}_{I,\beta} = f^J(\tilde{V}_\beta^I), \forall \beta, |\beta| = n, \beta_2 \leq r, \quad (5)$$

where $r \in \mathbb{Z}$, $0 \leq r \leq n-1$, and

$$\tilde{V}_\beta^I = \{\mathbf{t}'_{0,0}, \dots, \mathbf{t}'_{0,\beta_0-1}, \mathbf{t}'_{1,0}, \dots, \mathbf{t}'_{1,\beta_1-1}, \mathbf{t}'_{2,0}, \dots, \mathbf{t}'_{2,\beta_2-1}\}.$$

Equation (5) defines the affine relations between the control points of $\mathbf{F}^I(\mathbf{u})$ and $\mathbf{F}^J(\mathbf{u})$. Given a $r \in [0, n)$, let the control points satisfying Equation (5), then the discontinuity along certain knot lines disappear, and the curvature distribution along those lines improves. Figure 3 illustrates the case $r = 1$. For $\beta = (\beta_0, \beta_1, 1)$, Equation

(5) is written as

$$\begin{aligned} \mathbf{c}'_{(\beta_0, \beta_1, 1)} &= \frac{d(\mathbf{t}_{2,0}, \mathbf{t}_{1,\beta_1}, \mathbf{t}_{3,0})}{d(\mathbf{t}_{0,\beta_0}, \mathbf{t}_{1,\beta_1}, \mathbf{t}_{3,0})} \mathbf{c}'_{(\beta_0+1, \beta_1, 0)} \\ &+ \frac{d(\mathbf{t}_{0,\beta_0}, \mathbf{t}_{2,0}, \mathbf{t}_{3,0})}{d(\mathbf{t}_{0,\beta_0}, \mathbf{t}_{1,\beta_1}, \mathbf{t}_{3,0})} \mathbf{c}'_{(\beta_0, \beta_1+1, 0)} \\ &+ \frac{d(\mathbf{t}_{0,\beta_0}, \mathbf{t}_{1,\beta_1}, \mathbf{t}_{2,0})}{d(\mathbf{t}_{0,\beta_0}, \mathbf{t}_{1,\beta_1}, \mathbf{t}_{3,0})} \mathbf{c}'_{(\beta_0, \beta_1, 1)}, \end{aligned}$$

where $d(\cdot, \cdot, \cdot)$ is the determinant function. It is easy to verify that Equation (5) is just a linear combination of the control points for $0 \leq r \leq n-1$.

In the following, we consider the global fairing problem for triangular B -splines. Given a (planar, spherical or manifold) triangular B -spline surface $\mathbf{F}(\mathbf{u}) = \sum_I \sum_{|\beta|=n} \mathbf{c}_{I,\beta} N_{I,\beta}(\mathbf{u})$. We want to find a smooth surface $\tilde{\mathbf{F}}(\mathbf{u}) = \sum_I \sum_{|\beta|=n} \tilde{\mathbf{c}}_{I,\beta} N_{I,\beta}(\mathbf{u})$ such that $\tilde{\mathbf{F}}$ approximates the original surface \mathbf{F} as much as possible. This leads to the following least square problem:

$$\min_{\tilde{\mathbf{c}}} \sum_I \sum_{|\beta|=n} \|\tilde{\mathbf{c}}_{I,\beta} - \mathbf{c}_{I,\beta}\|^2 \quad (6)$$

$$\text{subject to } \tilde{\mathbf{c}}_{I,\beta} = f^J(\tilde{V}_\beta^I), \forall I, \forall \beta, |\beta| = n, \beta_2 \leq r$$

In the objective function, we minimize the squared distance between the control points of the original and the new spline surface, which implies that the minimal change of the shape. In the constraints, we use an integer r , $0 \leq r \leq n-1$, to control the smoothness of the spline surface. $r = 0$ implies that the control points along common edges of two adjacent triangles in the parametric triangulation are identical. The bigger value r , the smoother surface we will obtain. In our experiments, we can get visually pleasing surfaces with $r = 1$ or 2.

Since Equation (5) corresponds to affine relations between the control points of \mathbf{F}^I and \mathbf{F}^J , the constraints in Equation (6) are just linear equations of the control points. Therefore, Equation (6) is a linear constrained quadratic programming problem which has the following format:

$$\begin{aligned} \min_x \quad & \frac{1}{2} x^T Q x + c^T x + f \\ \text{subject to} \quad & A x = b \end{aligned}$$

Our problem is very special in that Q is an identity matrix. Therefore, it is very efficient to solve Equation (6) using Lagrange multiplier approach.

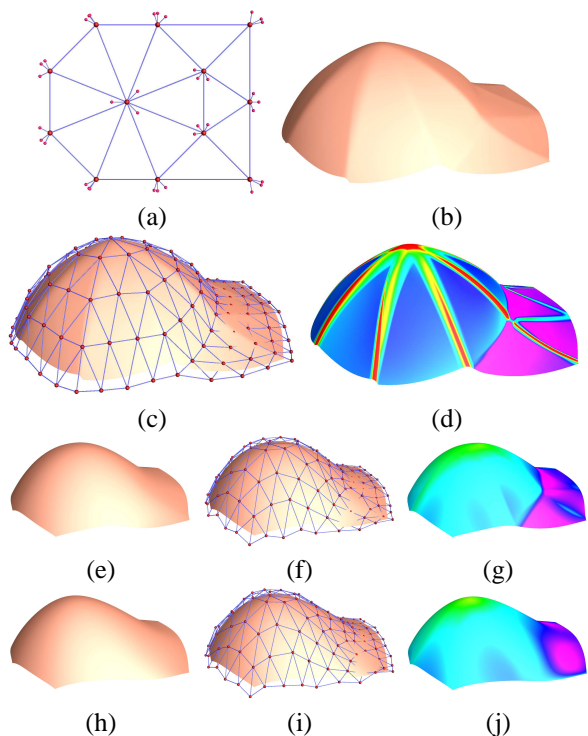


Figure 4: Illustration of our fairing algorithm to a degree 4 planar triangular B -spline: (a) shows the parametric domain. (Due to the shared control points of the spline surface, only three sub-knots have contribution to the shape.) (b) and (c) show the spline surface and the control net respectively. (d) shows the mean curvature of the spline surface. Note that the curvature along the image of the edges on the domain triangulation is significantly larger than the vicinity. (e)-(g) show fairing the spline surface with $r = 1$. (h)-(j) show fairing the spline surface with $r = 2$. Although the control points are not changed too much, the surface quality improves significantly.

5 EXPERIMENTAL RESULTS

We have implemented a prototype system on a 3GHz Pentium IV PC with 1GB RAM. We perform experiments on several models ranging from planar triangular B -splines to manifold triangular B -splines. Table 2 shows the spline configurations and execution times of our test cases.

Figure 4 illustrates the fairing algorithm to a planar triangular B -spline. Figure 5 shows example for fairing a spherical triangular B -spline. Compared to the shapes before and after fairing, the curvature concentration phenomena disappear, i.e., the knot-lines are eliminated.

Figure 6 shows examples of smooth triangular B -spline surfaces generated by our fairing algorithm. As shown in Figure 6, we can achieve highly smooth, e.g., C^3 and C^4 ,

Table 2: Statistics of test cases. n , degree of spline surface; N_t , # of domain triangles; N_c , # of control points; r , smoothness factor. The execution time measures in seconds.

Object	Type	n	N_t	N_c	r	Time
Cap	planar	4	13	123	2	< 1s
Face	planar	5	251	3181	2	2s
Venus	spherical	5	682	8527	2	8s
Skull	spherical	5	948	11852	2	16s
Dog	spherical	5	656	8202	2	7s
Foot	manifold	5	259	2139	2	1s
Bottle	manifold	3	1889	8513	1	6s

triangular B -spline surfaces of various topological types. These results demonstrate that triangular B -splines are both theoretic rigorous and feasible in practice.

6 CONCLUSION

In this paper, we have proposed an automatic and efficient method to generate visually pleasing, high-quality triangular B -splines of arbitrary topology. Our shape fairing technique works for planar, spherical, and manifold triangular B -splines. Our method is both fast and robust, as only a system of linear equations is solved. Furthermore, the shape deviation is minimized while the overall curvature distribution is significantly improved. Our experimental results on several real datasets have demonstrated that triangular B -splines are powerful and effective in both theory and practice.

ACKNOWLEDGEMENTS

This work was supported in part by the NSF grants IIS-0082035 and IIS-0097646, and an Alfred P. Sloan Fellowship to H. Qin and the NSF CAREER Award CCF-0448339 to X. Gu. The models are courtesy of Hugues Hoppe, Cindy Grimm, Michael Franssen, Cyberware, Headus, and New York University.

REFERENCES

- [1] P. Alfeld, M. Neamtu, and L. L. Schumaker. Bernstein-bezier polynomials on spheres and sphere-like surfaces. *Computer Aided Geometric Design*, 13(4):333–349, 1996.
- [2] P. Alfeld, M. Neamtu, and L. L. Schumaker. Fitting scattered data on sphere-like surfaces using spherical splines. *J. Comput. Appl. Math.*, 73(1-2):5–43, 1996.
- [3] C. L. Bajaj and I. Ihm. Smoothing polyhedra using implicit algebraic splines. In *SIGGRAPH '92*, pages 79–88, 1992.
- [4] W. Dahmen and C. A. Micchelli. Recent progress in multivariate splines. In C. Chui, L. Schumaker, and J. Ward, editors, *Approximation Theory IV*, pages 27–121. Academic Press, 1983.
- [5] W. Dahmen, C. A. Micchelli, and H.-P. Seidel. Blossoming begets B -spline bases built better by B -patches. *Mathematics of Computation*, 59(199):97–115, 1992.

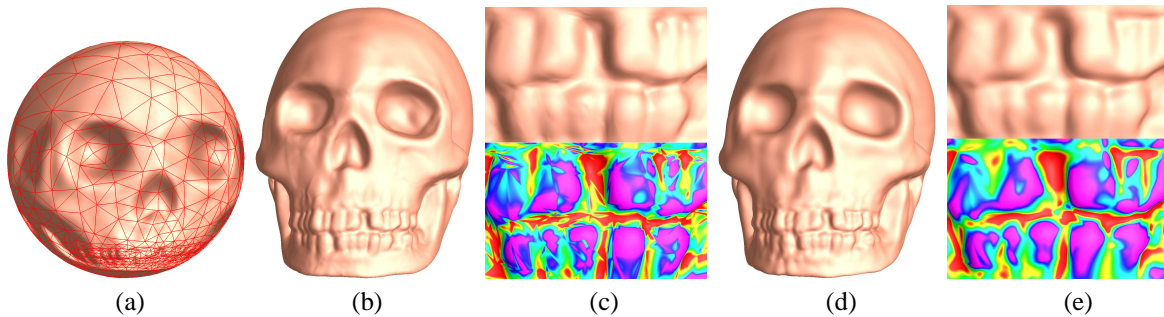


Figure 5: Illustration of our fairing algorithm for a spherical triangular B -spline: (a) A degree 5 spline with 948 patches. (b) The mean curvature of (a) (red, $H < 0$, cyan, $H > 0$, green, $H \approx 0$). Pay attention to the high curvature concentration along the image of edges of the spherical triangles. (d)-(e), After fairing, the curvature distribution improves significantly.

- [6] W. A. Dahmen and C. A. Micchelli. On the linear independence of multivariate B -splines. I. Triangulations of simploids. *SIAM J. Numer. Anal.*, 19(5):993–1012, 1982.
- [7] W. A. Dahmen and C. A. Micchelli. On the linear independence of multivariate B -splines. II. Complete configurations. *Math. Comp.*, 41(163):143–163, 1983.
- [8] C. de Boor. Splines as linear combinations of B -splines. A survey. In *Approximation theory, II (Proc. Internat. Sympos., Univ. Texas, Austin, Tex., 1976)*, pages 1–47. Academic Press, 1976.
- [9] M. Desbrun, M. Meyer, P. Schröder, and A. H. Barr. Implicit fairing of irregular meshes using diffusion and curvature flow. In *SIGGRAPH '99*, pages 317–324, 1999.
- [10] S. Fleishman, I. Drori, and D. Cohen-Or. Bilateral mesh denoising. *ACM Trans. Graph.*, 22(3):950–953, 2003.
- [11] P. Fong and H.-P. Seidel. An implementation of multivariate B -spline surfaces over arbitrary triangulations. In *Proceedings of Graphics Interface '92*, pages 1–10, 1992.
- [12] M. Franssen, R. C. Veltkamp, and W. Wesselink. Efficient evaluation of triangular B -spline surfaces. *Computer Aided Geometric Design*, 17(9):863–877, 2000.
- [13] I. Friedel, P. Mullen, and P. Schröder. Data-dependent fairing of subdivision surfaces. In *Proceedings of the eighth ACM symposium on Solid modeling and applications (SM '03)*, pages 185–195, 2003.
- [14] R. Gormaz. B -spline knot-line elimination and Bézier continuity conditions. In *Curves and surfaces in geometric design*, pages 209–216. A K Peters, 1994.
- [15] R. Gormaz and P.-J. Laurent. Some results on blossoming and multivariate B -splines. In *Multivariate approximation: from CAGD to wavelets (Santiago, 1992)*, volume 3 of *Ser. Approx. Decompos.*, pages 147–165. World Sci. Publishing, 1993.
- [16] G. Greiner and H.-P. Seidel. Modeling with triangular B -splines. *IEEE Computer Graphics and Applications*, 14(2):56–60, Mar. 1994.
- [17] X. Gu, Y. He, and H. Qin. Manifold splines. In *Proceedings of ACM Symposium on Solid and Physical Modeling (SPM '05)*, pages 27–38, 2005.
- [18] X. Gu and S.-T. Yau. Global conformal surface parameterization. In *Proceedings of the Eurographics/ACM SIGGRAPH symposium on Geometry processing (SGP '03)*, pages 127–137, 2003.
- [19] S. Hahmann. Fairing bicubic B -spline surfaces using simulated annealing. In A. L. Mehaute, L. L. Schumaker, and C. Rabut, editors, *Curves and Surfaces with Applications in CAGD*, pages 159–168. Vanderbilt University Press, 1997.
- [20] S. Hahmann. Shape improvement of surfaces. *Computing Suppl.*, 13:135–152, 1998.
- [21] M. Halstead, M. Kass, and T. DeRose. Efficient, fair interpolation using catmull-clark surfaces. In *SIGGRAPH '93*, pages 35–44, 1993.
- [22] Y. He, X. Gu, and H. Qin. Rational spherical splines for genus zero shape modeling. In *Proceedings of International Conference on Shape Modeling and Applications (SMI '05)*, pages 82–91, 2005.
- [23] Y. He and H. Qin. Surface reconstruction with triangular B -splines. In *Proceedings of Geometric Modeling and Processing*, pages 279–290, 2004.
- [24] K. Höllig. Multivariate splines. *SIAM J. Numer. Anal.*, 19(5):1013–1031, 1982.
- [25] S.-M. Hu, Y. Li, T. Ju, and X. Zhu. Modifying the shape of NURBS surfaces with geometric constraints. *Computer Aided Design*, 33(12):903–912, 2001.
- [26] M. Jin, Y. Wang, S.-T. Yau, and X. Gu. Optimal global conformal surface parameterization. In *Proceedings of IEEE Visualization (Vis '04)*, pages 267–274, 2004.
- [27] T. R. Jones, F. Durand, and M. Desbrun. Non-iterative, feature-preserving mesh smoothing. *ACM Trans. Graph.*, 22(3):943–949, 2003.
- [28] H. P. Moreton and C. H. Séquin. Functional optimization for fair surface design. In *SIGGRAPH '92*, pages 167–176, 1992.
- [29] M. Neamtu. Homogeneous simplex splines. *J. Comput. Appl. Math.*, 73(1-2):173–189, 1996.
- [30] M. Neamtu. Bivariate simplex B -splines: A new paradigm. In *Proceedings of the 17th Spring conference on Computer graphics (SCCG '01)*, pages 71–78, 2001.
- [31] R. Pfeifle and H.-P. Seidel. Fitting triangular B -splines to functional scattered data. In *Graphics Interface '95*, pages 26–33, 1995.
- [32] R. Pfeifle and H.-P. Seidel. Spherical triangular B -splines with application to data fitting. *Computer Graphics Forum*, 14(3):89–96, 1995.
- [33] L. Ramshaw. Blossom are polar forms. *Computer-Aided Geom. Design*, 6(4):323–358, 1989.
- [34] H.-P. Seidel. Symmetric recursive algorithms for surfaces: B -patches and the de Boor algorithm for polynomials over triangles. *Constr. Approx.*, 7:257–279, 1991.
- [35] H.-P. Seidel. Polar forms and triangular B -spline surfaces. In D.-Z. Du and F. Hwang, editors, *Euclidean Geometry and Computers, 2nd Edition*, pages 235–286. World Scientific Publishing Co., 1994.
- [36] G. Taubin. A signal processing approach to fair surface design. In *SIGGRAPH '95*, pages 351–358, 1995.
- [37] W. Welch and A. Witkin. Variational surface modeling. In *SIGGRAPH '92*, pages 157–166, 1992.

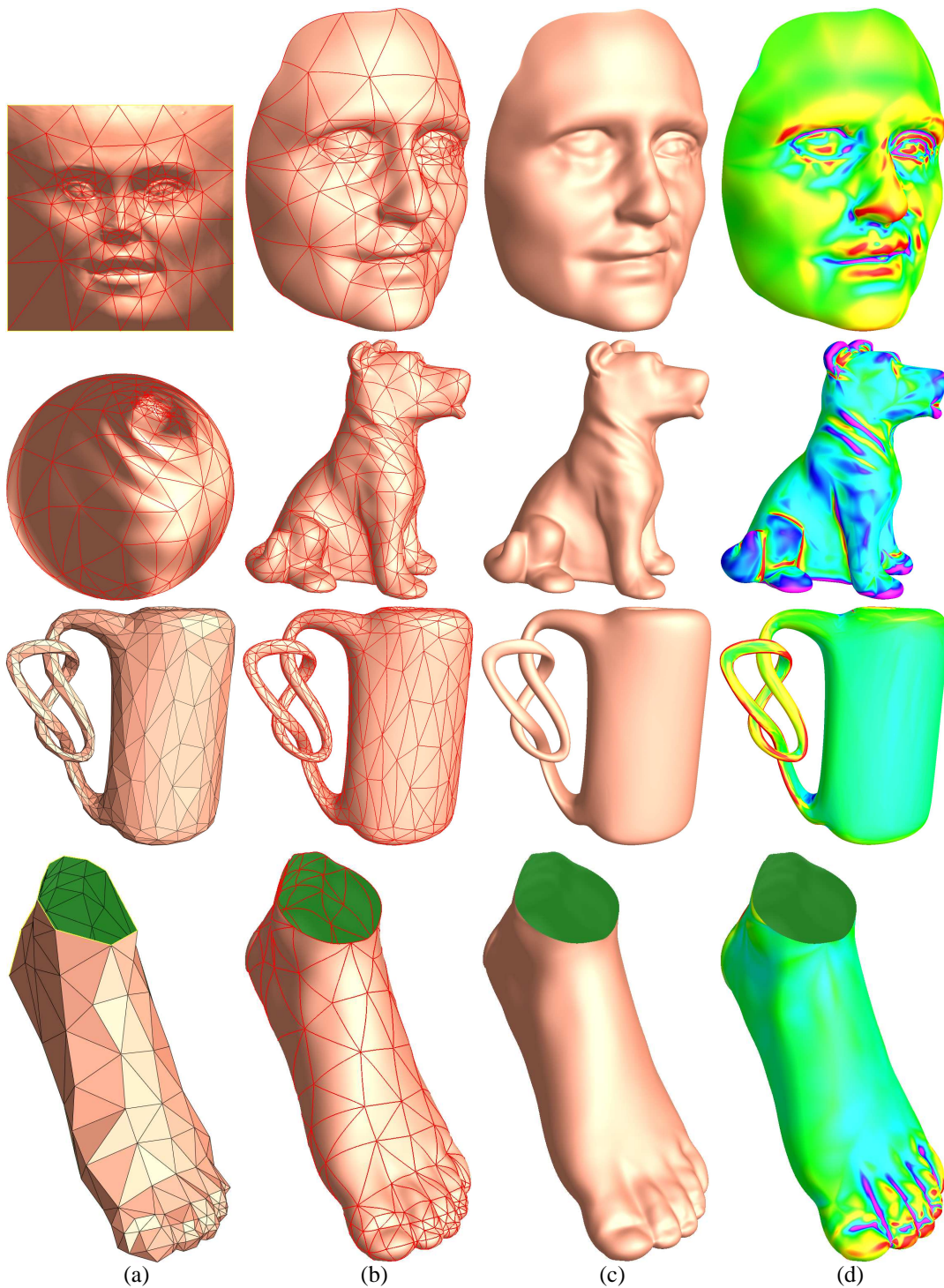


Figure 6: Examples of faired triangular B-splines. Row 1: a C^4 planar spline; Row 2: a C^4 spherical spline; Row 3: a C^2 manifold spline of genus 2 (The other handle is inside the bottle); Row 4: a C^4 manifold spline of genus 0 with boundaries. (a) shows the parametric domain. The red curves on the spline surfaces (b) correspond to the edges in the domain triangulation (a). (c) and (d) show the spline surfaces and mean curvature plots respectively. Note that there is no restriction on the triangulation of the parametric domain. Those knot-lines (curvature concentration on the image of the edges of domain triangulation) are completely eliminated.